2012-02-16

Optical Properties Of High Refractive Index Thin Films Processed At Low-Temperature

Mohamed Oubaha
Technological University Dublin, mohamed.oubaha@tudublin.ie

Salem Elmaghrum
Dublin City University

Robert Copperwhite
Dublin City University

Brian Corcoran
Dublin City University

Colette McDonagh
Dublin City University

Recommended Citation

Oubaha, M. et al. (2012) Optical Properties Of High Refractive Index Thin Films Processed At Low-Temperature, Optical Materials 34 (2012) 1366–1370 doi:10.1016/j.optmat.2012.02.023

Optical Materials 34 (2012) 1366–1370

Contents lists available at SciVerse ScienceDirect

Optical Materials

journal homepage: www.elsevier.com/locate/optmat

Optical properties of high refractive index thin films processed at low-temperature

Mohamed Oubaha [a,*], Salem Elmaghrum [b], Robert Copperwhite [a], Brian Corcoran [b], Colette McDonagh [a,c], Arnaud Gorin [a]

[a] Optical Sensors Laboratory, National Centre for Sensor Research, Dublin City University, Dublin 9, Ireland
[b] School of Mechanical and Manufacturing Engineering, Dublin City University, Dublin 9, Ireland
[c] Biomedical Diagnostics Institute (BDI), Dublin City University, Dublin 9, Ireland

ARTICLE INFO

Article history:
Received 10 November 2011
Received in revised form 10 February 2012
Accepted 16 February 2012
Available online 23 March 2012

Keywords:
Sol–gel
Hybrid materials
High refractive index
Optics
Photonics
Thin films

ABSTRACT

This study reports on the first development of high refractive index thin film materials processed at temperatures not greater than 100 °C. Three materials were synthesised by the sol–gel technique, each employing different transition metal precursors (niobium, tantalum and vanadium alkoxides). The optical properties of these materials were characterised by ellipsometry and the propagation losses at 638 nm were measured by the prism coupling method. It is shown that refractive indices as high as 1.870, 2.039 and 2.308 are obtained from niobium-, tantalum- and vanadium-based materials respectively, attributed to the influence of the transition metal atomic size on the condensation reactions.

1. Introduction

Many technologies in photonics use high refractive index thin film materials (typically >1.65) to improve the performance of optical devices such as Brag gratings [1], waveguide-based optical circuits [2], and photonic crystals [3]. In photovoltaic applications, anti-reflection coatings comprising high refractive index thin films are used in solar cells to trap the incident light and increase the amount of light coupled into the solar cell [4,5]. In waveguide-based optical sensors, it has been demonstrated that a high refractive index superstrate layer on the waveguide surface results in lower limits of detection [6,7]. In integrated optical devices, multilayer thin films with high refractive index contrast are extensively used for the fabrication of optical interference filters and mirrors [8,9]. In addition to high refractive index, important requirements for high refractive index materials include high optical quality and transparency over the visible spectral range. Film thickness control is also critical and the optimum thickness depends on the refractive index value and is usually between 30 and 150 nm [6–9]. Furthermore, a low temperature deposition process is frequently desirable to facilitate the integration of different optical components on substrates such as glass or plastic.

High refractive index layers are usually obtained with metal oxide materials. Metal oxide materials such as TiO_2 or Ta_2O_5 exhibit refractive index values above 1.8 and are transparent in the visible range. These materials are often deposited through evaporation or sputtering. Unfortunately, these methods are not only expensive, but post-deposition high temperature treatments are often necessary to obtain good adhesion and good optical properties [10].

Hybrid organic–inorganic sol–gel materials based on metal oxides have been proposed as an alternative to conventional materials. They are composed of both organic and inorganic moieties, which can be covalently bound or stabilized within the same matrix via the presence of electrostatic interactions [11]. Due to the possibility of precisely controlling the content of each moiety, it has been possible to develop materials exhibiting an optimum combination of mechanical, optical and thermal properties. Hybrid organic–inorganic materials are promising candidates for the low cost fabrication of high refractive index materials with good optical quality because they offer the possibility to combine the high refractive index of bulk metal oxides with the low temperature processing conditions typical of sol–gel derived materials.

Most hybrid materials reported in the literature are based on ZrO_2 and TiO_2 metal oxides [12–15]. However, though these metal oxides give rise to hybrid materials with excellent optical properties, they are generally obtained after annealing at high temperature (>400 °C) [11,12], which is incompatible with many device fabrication processes. Recently, we reported a low temperature ZrO_2 based hybrid material with a refractive index of 1.746 after

* Corresponding author.
E-mail address: am.oubaha@gmail.com (M. Oubaha).

0925-3467/$ - see front matter © 2012 Elsevier B.V. All rights reserved.
doi:10.1016/j.optmat.2012.02.023

100 °C annealing [16]. This process for fabrication of high refractive index thin films satisfies the key requirements for many applications, namely; low temperature processing; low surface roughness; high transparency.

In this paper, we propose the development of a low temperature route for the deposition of high refractive index thin films based on niobium, tantalum and vanadium alkoxides. In order to obtain transparent and homogenous solutions an original multi-step sol–gel synthesise has been developed and thoroughly described in the experimental section. The structure, morphology and thermal behaviour of the developed materials has been characterised by XRD, Raman spectroscopy, TEM and TGA. Optical characterisations including ellipsometry and propagation loss measurements employing the prism coupling method of the developed thin films are proposed and the obtained results are discussed.

2. Experimental

2.1. Materials development

The objective was to prepare transparent and homogeneous transition metal oxide-based thin film materials from the following niobium, tantalum and vanadium alkoxide precursors: niobium ethoxide (99.95%), Sigma–Aldrich; tantalum ethoxide (99.98%), Sigma–Aldrich; and vanadium tri-isopropoxide, (>98%) Strem. The synthesis employed here is the hydrolytic sol–gel route, which involves hydrolysis and condensation reactions resulting in the formation of a metal oxide three-dimensional network. The syntheses were performed in a three step process: (1) formation of hybrid complexes by chelation of the metal alkoxide precursors, (2) dilution of the hybrid complexes; (3) hydrolysis and condensation of the hybrid complexes. To avoid the formation of undesired agglomerates during the hydrolysis reaction, a chelating agent was utilised to decrease the reactivity of the employed metal alkoxide precursors. This was achieved by addition of a strong complexing ligand to the alkoxide [11]. In this study, methacrylic acid (MAA, Sigma–Aldrich, 99%) was employed as the complexing ligand. This caused the formation of hybrid complexes in which the number of reactive alkoxide groups is decreased, thereby making this precursor less reactive to hydrolysis. In order to obtain the highest possible refractive index without the performance of a high temperature post-bake heat treatment, the chelating agent concentration must be minimal. Such a compromise was found with 1 mol.% of MAA with respect to the transition metal alkoxide concentration for all materials. In order to further slow down the condensation kinetics of the hybrid complex and allow precise control of the film thickness, a dilution step was performed after 1 h of reaction employing isopropanol (IPA, Sigma–Aldrich, 99%) with a volume ratio of 1:15/hybrid complex:IPA. Following another hour of reaction, the hydrolysis step was performed utilising pH 7 deionized water with a molar ratio of 1:10 with respect to the metal transition alkoxide precursor. Prior to hydrolysis, the deionized water was diluted 500 times with IPA to prevent any formation of agglomerates. For example, the tantalum solution was prepared by mixing thoroughly 3.5 g (8.6×10^{-3} mol) of tantalum ethoxide with 0.008 g (9.3×10^{-5} mol) of MAA, followed by the addition of 35 ml of IPA. The hydrolysis was performed by mixing 0.07 g of H_2O with 35 ml of IPA. All sols were synthesised under the same conditions and left stirring for 24 h before use. Therefore, the lifetime of the sols has been observed to be strongly relying on the storage temperature and age of the materials. At ambient temperature, after three to four days of ageing, precipitates resulting from the agglomeration of inorganic species are clearly visible. However, when the sols are stored at temperatures not greater than 0 °C, the lifetime of the sols exceeds three months, which can be attributed to the strong decrease of the condensation kinetic limiting thermal mobility of the reactive inorganic groups.

2.2. Instrumentation

2.2.1. Materials characterisation techniques

Raman spectroscopy was performed using a Perkin Elmer® 60 Raman Station 400F.

The structural characterisation of all samples was carried out by (D8 ADVANCE-BRUKER) X-ray diffraction (XRD) using Cu Kα radiation. The machine is connected to a computer with a package of associated softwares called DIFFRAC PLUS Evaluation.

Thermo-gravimetric analysis (TGA) was carried out in air to estimate the temperatures at which the decomposition and oxidation of the organic ligand take place.

The morphology of the materials was observed by a transmission electron microscope (TEM, Philips CM 20, Eindhoven, The Netherlands).

2.2.2. Optical characterisations

The hybrid materials based on the three different transition metal alkoxides (niobium, tantalum and vanadium) were deposited by spin-coating on glass and silicon substrates to form transparent thin films, and heat treated at 100 °C for 1 h for the final stabilization of the layer.

Optical measurements were performed using ellipsometry and transmission measurements in order to determine the performance of the materials. Transmittance spectra and ellipsometry measurements were conducted over the 400–900 nm spectral range. Thickness and refractive index of the films were calculated using the Tauc–Lorentz model fitted to the ellipsometry data [17]. In order to characterise the propagation losses, thin films were deposited on silicon substrates with a thick optical isolation layer. A ZrO_2 based hybrid material with a refractive index around 1.5 and a thickness of 6 μm was chosen as the optical isolation layer due to its low absorption in the visible range and its well-known optical properties [18]. The thickness of the obtained hybrid thin films was specified at 100 nm for single-mode waveguiding, in accordance with beam propagation method calculations (OlympiOs, C2V Netherlands). The thickness of the films was controlled primarily by the rotating speed of the spin-coater during deposition.

Optical propagation losses measurements in the planar waveguides were conducted using a polarisation maintaining fibre (TE mode) coupled laser diode at 638 nm. Light was coupled into the waveguides using a high refractive index TiO_2 prism. Propagation losses were estimated from the exponential profile of the scattering losses from the surface of the waveguides as a function of propagation distance, using a high resolution CCD camera [17].

3. Results and discussion

XRD patterns shown in Fig. 1 were performed in order to identify the crystalline structure of the developed materials to allow comparison with structures obtained with conventional techniques prepared at high temperatures, leading to crystallised oxide materials (Ta_2O_5, Nb_2O_5 and V_2O_5). In comparison with patterns of these crystallised oxides [19–21], where clear crystallisation peaks can be seen in the investigated 2θ range, one can observe that our materials do not exhibit any well-identified crystallisation peaks, demonstrating their amorphous character. This can be attributed to two parameters: first, the low temperature process that does not seem to be sufficient to allow the formation of stoichiometric oxides usually accompanied by a crystallisation process; second the presence of an organic ligand, which is probably still present

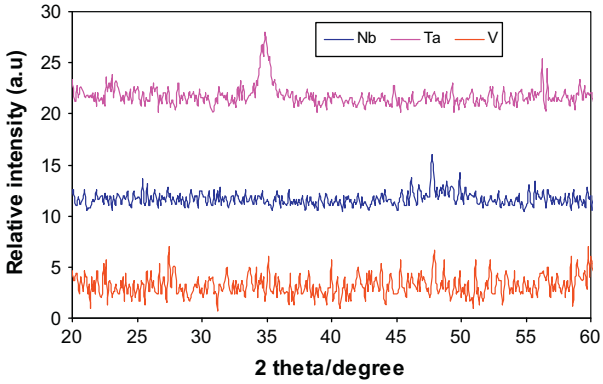

Fig. 1. XRD patterns of niobium-, tantalum and vanadium hybrid materials.

after this low temperature baking. To clarify this, it has been decided to analyse the structure of the materials by Raman spectroscopy. As Raman spectra of the 3 materials investigated here exhibit similar behavior, we have decided to only present and discuss the spectrum of the tantalum based material. Fig. 2 represents the Raman spectrum of the tantalum-based material. The strongest Raman signals are located in the CH stretching region (2800–3000 cm^{-1}), assigned to the CH stretching vibrations of the MAA alkyl chain demonstrating the presence of organic moieties after a heat treatment at 100 °C for one hour and consequently allowing to consider these systems as hybrid materials. The band located at 1640 cm^{-1} corresponds to the deformation of the water molecule. This proves that the materials still contain traces amount of water. The ν (C—O) band at 924, 858 and 976 cm^{-1} can be assigned to the bending mode of a bridging acetate group in a bidentate configuration of tantalum. In addition, the COO^- rocking and deformation modes are apparent as a single band centred at 600 cm^{-1}. In conjunction with the absence of any strong band around 1680 cm^{-1} related to carbonyl bonds (C═O), these observations confirm that the entire amount of MAA is utilised in the chelation of the tantalum by the acetate groups, as described previously [22]. The tantalate bonds (Ta—O—Ta) resulting from the sol–gel hydrolysis and condensation reactions can clearly be seen in the regions of 400–950 cm^{-1} as well as the deformation of the C—C bands at 276 cm^{-1}. All other Raman signals are summarised in Table 1.

The XRD and Raman characterisations demonstrated the formation of amorphous materials, which has been associated to the low-temperature preparation process that allow the presence of the organic ligand in the final materials. However, it would be of a great interest to investigate the morphology of the thin film materials and the effect of the heat treatment on the stability of

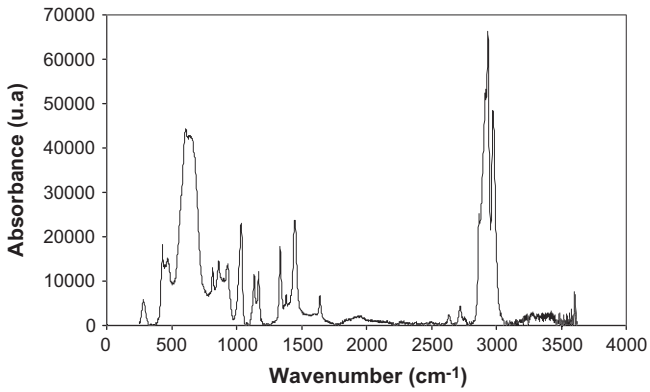

Fig. 2. Raman spectrum of tantalum material.

Table 1
Assignment of Raman.

2976–2918	ν (C—H) [CH_2; CH_3]
1640	δ (H_2O)
1444; 1380; 1334	δ (CH) [CH_2; CH_3]
1168; 1131; 1032	ν (C—O—Ta)
924; 858; 814	ν (C—O)
600	ν (O—C—O^-)
462; 426	ν (O—Ta—O)
278	δ (C—C)

the materials. TEM images recorded on the prepared materials are shown in Fig. 3. From these images, it seems difficult to identify any difference in the particle sizes. However, one can observe that the tantalum-based material exhibit a much higher homogeneity with no observation of any micro-cracks or porosity. The niobium- and vanadium-based materials seem to produce rough surfaces with appearance of meso- and micro-pores, respectively. This could be associated to different hydrolysis and condensation kinetics leading to the faster formation of the inorganic network, resulting in the appearance of porous structures. TGA curves of all samples exhibited a similar tendency as represented in Fig. 4 by the tantalum-based sample. Over the temperature range 25–900 °C, the TGA curve exhibits a slow quasi-linear decrease up to 150 °C with a loss of 0.5% of its initial weight, then a strong decrease up to 250 °C with an additional loss of matter of 2%, followed by a quasi-stagnation (decrease <0.5%) of the weight up to 900 °C. This three-step behaviour typically symbolises the subsequent removal of the residual and adsorbed water, the decomposition of the organic acid (that generally occur above 150 °C) into carbon dioxide and water, as well as the crystallisation of the material (usually taking place at temperature over 500 °C, without significant loss of matter). These results converges in confirming the hybrid nature of our materials, due to the presence of organic moieties at temperatures not greater than 100 °C, and a higher homogeneity for the tantalum material in comparison with the niobium- and vanadium-based materials.

Fig. 5 shows the variation of the refractive index as a function of the wavelength for the three different metal oxide compositions investigated here. Normal dispersion curves were obtained, with higher refractive index values for lower wavelength. Refractive indices of 1.870, 2.039 and 2.308 were measured at 635 nm for tantalum, niobium and vanadium hybrid thin films, respectively. The samples were stored both under ambient atmosphere and in humidity-free environment for a period of ten weeks and the refractive index values were found to remain constant within the error bar measurement (±0.005), demonstrating the good stability of the materials.

The difference in the refractive index value of these materials can be explained by the ability of the metal transition to condense and form large clusters or possibly agglomerates during the sol–gel synthesis, the deposition and the final thermal stabilization, as previously confirmed by the TEM images. As the three transition metals employed here exhibit similar physico-chemical properties (electron configuration, oxidation states, atomic radius, electronegativity), it is anticipated that the main parameter governing the condensation process is the atomic size, which can be correlated with the measured refractive indices. Indeed, the smaller the atomic size, the higher the refractive index suggesting that the condensation process of the oligomeric species into larger clusters is facilitated by smaller molecules. This hypothesis is supported by the fact that polycondensation reactions in sol–gel chemistry require accessibility to the active hydroxide sites. This access is dependent on steric hindrance which can be caused by the presence of large atoms such as transition metals, thereby limiting the polycondensation reaction propagation. To our knowledge, this

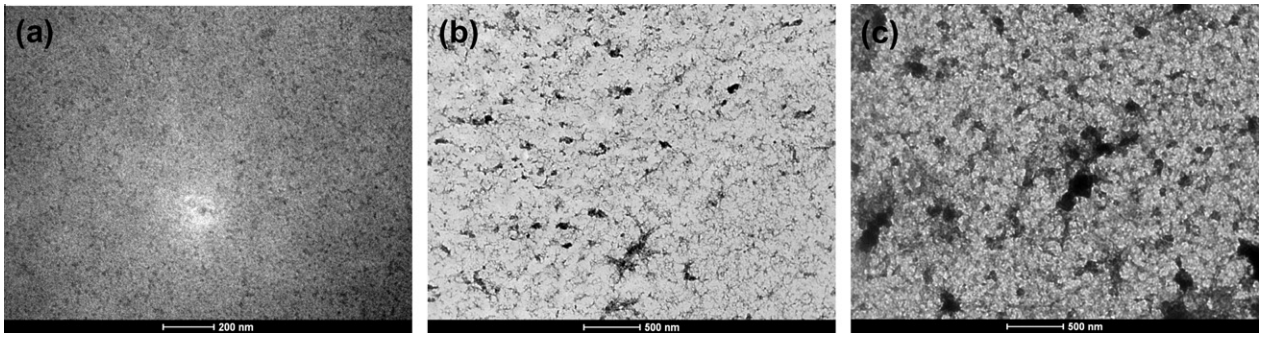

Fig. 3. TEM images of tantalum (a), niobium (b) and vanadium (c) hybrid materials.

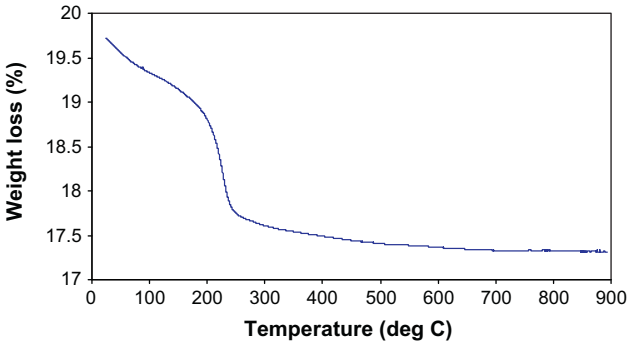

Fig. 4. TGA analysis of tantalum material.

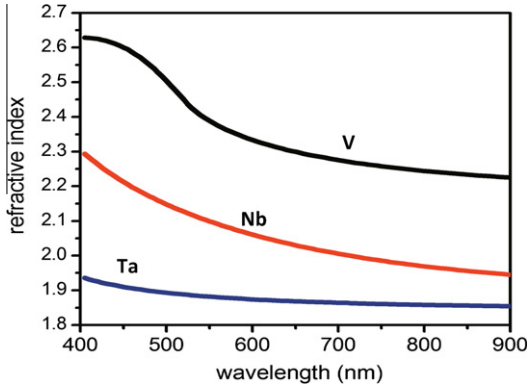

Fig. 5. Refractive index of the niobium-, tantalum and vanadium hybrid materials versus the wavelength in the visible range.

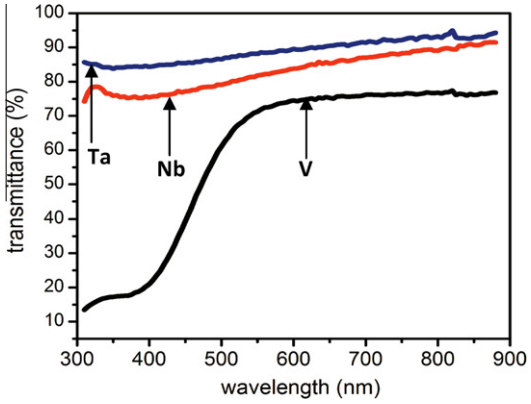

Fig. 6. Transmission spectra of niobium-, tantalum and vanadium hybrid materials.

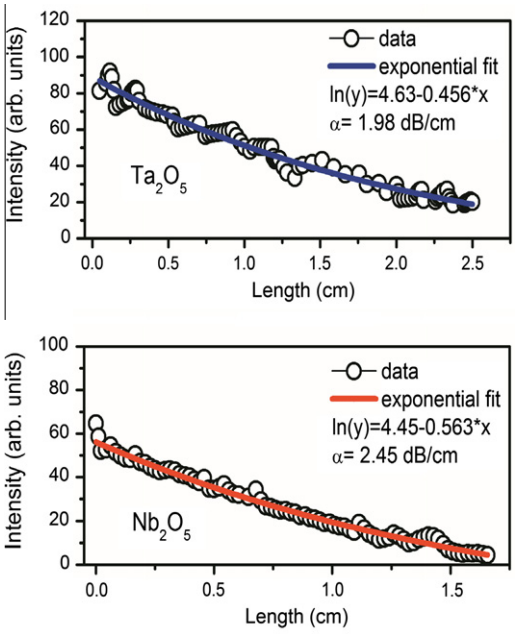

Fig. 7. Results of top-side surface measurements of scattered light intensity along propagation axis of the planar waveguides fabricated with hybrid materials based on Ta_2O_5 and Nb_2O_5.

essential physico-chemical sol–gel phenomenon has not been highlighted before and complementary investigations are ongoing in our group to confirm the fundamental chemistry of this phenomenon.

The transmission spectra in the visible range of the developed materials deposited on glass are plotted in Fig. 6. For comparison purposes, the thickness of the three samples was adjusted to 100 nm. One can observe that the transmission spectra strongly depend on the nature of metal oxide that has been incorporated into the hybrid material. The highest transmission is obtained with the tantalum based material, followed by niobium and vanadium, with transmission values at 635 nm of around 90%, 85% and 75%, respectively. It is important to note that after deposition and thermal stabilization of all films, the vanadium-based hybrid thin film was yellowish in comparison with the two other samples which were colourless. It is well known that colour changes of transition metal-based materials are due to a modification of the number of electrons in the d orbitals of the transition metal [23]. Here, the most plausible explanation of yellowing is that the molecule of water released during the sol–gel condensation reactions (V—OH + V—OH → V—O—V + H_2O) is re-utilised in the hydrolysis

of the vanadium precursor, leading to larger oligomers in which the number of electrons in the d orbitals of the vanadium atom is significantly increased explaining both the colour change of the vanadium based thin film and reinforcing the hypothesis proposed earlier regarding the reactivity of the vanadium precursor.

Loss measurements based on measurement of the scattered light profile in planar waveguides (638 nm – TE polarised light) containing tantalum and niobium are shown in Fig. 7. It was impossible to measure the losses in the hybrid material containing vanadium since no light could be propagated into the waveguide. This is probably due to the strong visible absorption that has been observed in the transmission measurement. The propagation losses of niobium-based waveguides were measured to be 2.45 dB/cm, while the tantalum-based waveguides exhibited slightly lower losses of 1.98 dB/cm. Propagation losses are well-known to result from the addition of the materials absorptions, inherent to the molecular vibrations, and the light scattering, due to the morphology and particle size. From both the transmission results and TEM images, the tantalum-based materials exhibit the most favourable transparency and homogeneity, which can therefore explain the higher propagation performances Therefore, these propagation losses are comparable to those reported in the literature for hybrid materials containing ZrO_2 or TiO_2 [14,15].

4. Conclusion

In summary, the optical properties of hybrid thin films synthesised from three different transition metal alkoxides were compared. It was found that the hybrid material containing tantalum had lower optical propagation losses than the one containing niobium. No light could be propagated into the waveguide containing vanadium, probably due to the strong absorption of the vanadium in the visible range. Niobium or tantalum hybrid-based materials are promising solutions for the development of low cost and low temperature processed photonic devices with high optical performance and high refractive index. Finally, this study has in particular highlighted a fundamental phenomenon regarding the relationship between the material condensation and the nature of the transition metal which we strongly believe this will open the way to further key investigations in sol–gel science.

References

[1] A. Cusano, A. Iadicicco, D. Paladino, S. Campopiano, A. Cutolo, M. Giordano, Optical Fiber Technology 13 (2007) 291–301.
[2] W.F. Ho, M.A. Uddin, H.P. Chan, Polymer Degradation and Stability 94 (2009) 158–161.
[3] Tomas Kohoutek, Jiri Orava, Tsutomu Sawada, Hiroshi Fudouzi, Journal of Colloid and Interface Science 353 (2011) 454–458.
[4] J. Hu, R.G. Gordon, Solar Cells 30 (1991) 437.
[5] C. Leguijt, P. Lok Igen, J.A. Eikelboom, A.W. Weeper, F.M. Schuurmans, W.C. Sinke, P.F.A. Alkemade, P.M. Sarro, C.H.M. Maree, L.A. Verhoef, Solar Energy Materials and Solar Cells 40 (1996) 297.
[6] R. Bernini, N. Cennamo, A. Minardo, L. Zeni, IEEE Sensors Journal 6 (2006) 1218.
[7] G. Stewart, F.A. Muhammad, B. Culshaw, Sensors and Actuators B–Chemical 11 (1993) 521–524.
[8] C. Richard, A. Renaudin, V. Aimez, P. Charette, Lab on a Chip 9 (2009) 1371.
[9] N. Kim, J.F. Stebbins, Chemistry of Materials 23 (15) (2011) 3460–3465.
[10] B.S. Ahluwalia, A.Z. Subramanian, O.G. Helleso, N.M.B. Perney, N.P. Sessions, J.S. Wilkinson, IEEE Photonics Technology Letters 21 (2009) 1408.
[11] J. Livage, C. Sanchez, Journal of Non-Cryst Solids 145 (1992) 11.
[12] R. Chassagnon, O. Marty, P. Moretti, C. Urlacher, J. Mugnier, Nuclear Instruments and Methods in Physics Research, Section B, 122 550 (1997).
[13] C. Urlacher, J. Dumas, J. Serughetti, J. Mugnier, M. Munoz, Journal of Sol–Gel Science and Technology 8 (1997) 999.
[14] M. Bedu, G. Sagarzazu, T. Gacoin, P. Audebert, C. Weisbuch, L. Martinelli, Thin Solid Films 518 (2010) 4450.
[15] R. Himmelhuber, P. Gangopadhyay, R.A. Norwood, D.A. Loy, N. Peyghambarian, Optical Materials Express 1 (2) (2011) 252–258.
[16] A. Gorin, R. Copperwhite, S. Elmaghrum, C. Mc Donagh, M. Oubaha, Proceedings SPIE 8191 (2011).
[17] A. Gorin, A. Jaouad, E. Grondin, V. Aimez, P. Charette, Optics Express 16 (2008) 13509.
[18] M. Oubaha, M. Smaihï, P. Etienne, P. Coudray, Y. Moreau, Journal of Non-Crystalline Solids 318 (2003) 305–313.
[19] Guolong Guo, Jianhua Huang, Materials Letters 65 (2011) 64–66.
[20] Lin Chen, Qing-Qing Sun, Jing-Jing Gu, Yan Xu, Shi-Jin Ding, David Wei Zhang, Current Applied Physics 11 (2011) 849–852.
[21] I. Quinzeni, S. Ferrari, E. Quartarone, P. Mustarelli, Journal of Power Sources 196 (2011) 10228–10233.
[22] G. Ehrhart, B. Capoen, O. Robbe, P. Boy, S. Turrell, M. 70, Bouazaoui, Thin Solid Films 496 (2006) 227–233.
[23] Antonin Vlcek Jr., Stanislav Zalis, Coordination Chemistry Reviews 251 (2007) 258–287.